Three-dimensional distortions of the tokamak plasma boundary: boundary displacements in the presence of saturated MHD instabilities

Three-dimensional distortions of the tokamak plasma boundary: boundary displacements in the presence of saturated MHD instabilities

I.T. Chapman[1], D. Brunetti[2], P. Buratti[3], W.A. Cooper[2], J.P. Graves[2], J.R. Harrison[1], J. Holgate[1,4], S. Jardin[5], S.A. Sabbagh[6], K. Tritz[7], the MAST and NSTX Teams and EFDA-JET Contributors[a]

[1] EURATOM/CCFE Fusion Association, Culham Science Centre, Abingdon, Oxon, OX14 3DB, UK

[2] CRPP, Association EURATOM/Confédération Suisse, EPFL, 1015 Lausanne, Switzerland

[3] Associazione EURATOM-ENEA sulla Fusione, CR Frascati, Roma, Italy

[4] Cavendish Laboratory, Department of Physics, University of Cambridge, J J Thomson Avenue, Cambridge, CB3 0HE, UK

[5] PPPL, Princeton University, PO Box 451, Princeton, NJ 08543, USA

[6] Department of Applied Physics and Applied Mathematics, Columbia University, New York, USA

[7] Johns Hopkins University, Baltimore, MD, USA

E-mail: ian.chapman@ccfe.ac.uk

Abstract

The three-dimensional plasma boundary displacement induced by long-lasting core magnetohydrodynamic (MHD) instabilities has been measured in JET, MAST and NSTX. Only saturated instabilities are considered here since transient rapidly growing modes which degrade confinement and act as potential triggers for disruptions bring more fundamental concerns than boundary displacements. The measured displacements are usually small, although in extreme cases in MAST when the rotation braking is strong, a significant global displacement can be observed. The instability most likely to saturate and exist for many energy confinement times whilst distorting the boundary of ITER is the saturated internal kink, or helical core, which can be found in plasmas with a wide region of low magnetic shear such as the hybrid scenario. This mode can lead to non-negligible boundary displacements. Nonetheless, the boundary displacement resultant from core MHD instabilities in ITER is predicted to be less than $\pm 1.5\%$ of the minor radius, well within tolerable limits for heat loads to plasma-facing components.

Keywords: non-axisymmetry, 3d displacements, saturated MHD instabilities

(Some figures may appear in colour only in the online journal)

1. Introduction and background

There are various conditions under which fusion plasmas are susceptible to long-lasting plasma instabilities which can give rise to displacements of the plasma boundary. For the purposes of this study, we discount any displacements arising due to transient events since these distortions are especially hard to model numerically and therefore extrapolation of probable distortions in ITER is problematic. It has been observed in many devices that in plasmas with a wide region of low magnetic shear and $q \geqslant 1$, the plasma exhibits long-lasting $n = 1$ ideal magnetohydrodynamic (MHD) instabilities [1–7]. Similarly, neoclassical tearing modes can exist for multiple energy confinement times [2, 10–12] and resistive wall modes (RWMs) controlled by magnetic feedback can also be sustained for a long time [13–16]. Routinely, the boundary displacement due to such instabilities is of secondary concern, even though it does lead to a noticeable level of non-axisymmetry and can cause large displacements under certain conditions.

However, such perturbations to the boundary could lead to unacceptable heat loads on the plasma-facing components in ITER. The allowable plasma displacement to avoid damage to the first wall has been assessed as 8 cm with three-dimensional scrape-off layer transport modelling [17], whilst the boundary

---

[a] See the appendix of Romanelli F. *et al* 2012 *Proc. 24th Int. Conf. on Fusion Energy 2012 (San Diego, CA, 2012) (Vienna: IAEA).* (www-naweb.iaea.org/napc/physics/FEC/FEC2012/index.htm)

must stay within a 4 cm envelope of its set point to achieve good RF coupling [18]. Consequently it is important that we can predict the likely distortions in ITER and prepare methods for the avoidance or control of such boundary displacements. This paper documents the displacement of the plasma edge due to saturated core instabilities for the first time.

Measurements of the displacements caused by core MHD are described in section 2 and compared to numerical modelling in section 3. Then predictions for the displacements expected in ITER due to core MHD are made in section 4 before the implications of the work are discussed in section 5.

2. Measurements of displacements due to core MHD in present machines

2.1. Internal $n/m = 1/1$ kink modes

In this section we are only concerned by edge displacements due to saturated core MHD instabilities. Edge displacements have been measured with the multi-energy soft x-ray (ME-SXR) system on NSTX in the presence of core-localized $n = 1$ internal kink and tearing modes. The ME-SXR cameras have 1 cm radial resolution between channels near the plasma edge, and interpolation allows sub-cm resolution. An $n = m = 1$ internal kink mode in plasmas with low shear above $q = 1$ has been found to couple to $m/n = 2/1$ tearing modes, giving rise to islands of 10 cm, equating to 15% of the minor radius [19]. The position of the boundary in the presence of a 1/1 kink coupled to a 2/1 tearing mode as measured by the ME-SXR system, which can persist for half the length of the plasma discharge in NSTX, is illustrated in figure 1. It is evident that the plasma boundary is distorted by ±0.75 cm, or ±1.3% of the minor radius.

MAST plasmas with a safety factor above unity and a profile with either weakly reversed shear, or broad low-shear regions, regularly exhibit long-lived saturated ideal MHD instabilities [1]. The toroidal rotation is flattened in the presence of such perturbations and the fast ion losses are enhanced [20]. These ideal long-lived modes (LLMs), distinguished as such by the notable lack of islands or signs of reconnection, are driven unstable as the safety factor approaches unity. This could be of significance for advanced scenarios, or hybrid scenarios which aim to keep the safety factor just above rational surfaces associated with deleterious resistive MHD instabilities, especially in spherical tokamaks which are susceptible to such ideal internal modes for q_{min} further above a rational surface than conventional aspect ratio devices.

Under typical circumstances the long-lived kink mode (LLM) seen in MAST plasmas with broad low-shear q-profiles [1] does not significantly perturb the plasma boundary, although the plasma core does undergo multi-cm oscillations [20, 21]. However, there are circumstances under which significant edge perturbations are observed. For instance, figure 2 shows the D_α light measured by the fast visible camera as a function of tangency radius at the midplane in MAST in the presence of an $n = 1$ kink mode. As the mode rotates past the field of view of the camera, the plasma boundary moves in and out by 3–4 cm, equating to 4–6.5% of the minor radius. Here, the exposure time of the camera was $2\,\mu$s whilst the temporal
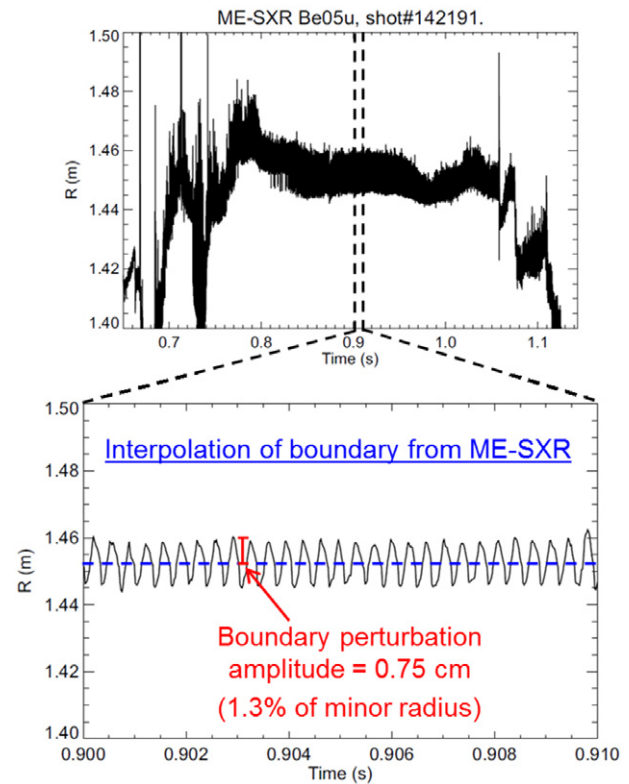

Figure 1. The plasma boundary measured by the ME-SXR system in NSTX for a discharge with a core saturated 1/1 kink mode coupled to a 2/1 tearing mode, showing a displacement of 1.3% of the minor radius.
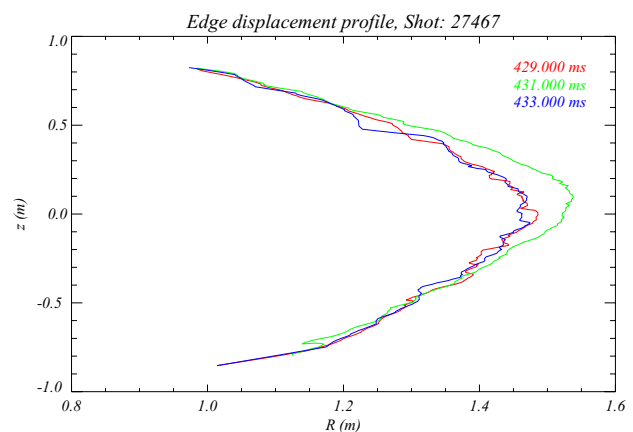

Figure 2. The plasma boundary measured by high-speed visible imaging in MAST showing the distortions in the presence of saturated core MHD activity.

resolution was 500 Hz. The spatial resolution is approximately 0.3 cm. The CCD camera directly images visible light photons using a wide field of view lens. The camera location was determined by reference to the location of known features inside the vessel in the image plane and within a 3D co-ordinate system with MAST at its centre. The camera location and field of view then allow the radius at which camera lines of sight are tangent to flux surfaces to be calculated, giving the local plasma brightness as a function of radius. The boundary is found using the part of the camera image from the X-point
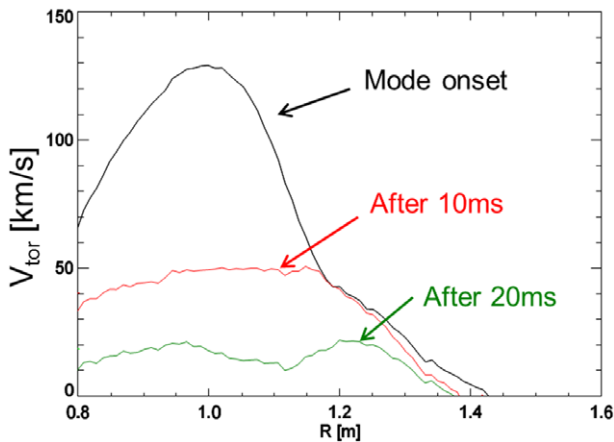
Figure 3. The plasma toroidal velocity profile measured by charge exchange recombination spectroscopy in MAST. The rotation profile in black is at the time at which the LLM is first observed, the red profile is after 10 ms, whilst the green profile is after 20 ms and is the profile occurring at the time at which boundary shape is given by the green profile in figure 2.

Figure 4. The edge displacement in MAST as a function of the toroidal velocity at the radial position of the minimum in safety factor.

going outboard, and finding the maximum brightness for each row of pixels in the camera image, and recording the (R, Z) location of where the brightest pixel is tangent to circular flux surfaces. When the plasma is rotating quickly, the distortion is confined to the plasma core, whereas at low rotation, the plasma boundary can become significantly perturbed. Often, such large distortions lead to plasma terminations, though there are rare occasions when the plasma survives and the safety factor evolution results in the decay of the mode.

Figure 3 shows how the core plasma rotation profile is degraded by the presence of a LLM. Such strong rotation braking was attributed to the neoclassical viscous torque arising from the non-axisymmetry introduced by the $n = 1$ core distortion [20, 22]. The saturated amplitude of the mode was estimated by comparing experimental SXR data to simulations for different eigenstructure amplitudes, enabling the calculation of the braking torque according to the NTV theory [23]. The result is in good accordance with the measured braking, except at rational surfaces [20, 22]. Here, the mode's eigenstructure is expected to be intransigent as it saturates [24, 25], and the effect of enhanced fast ion losses is neglected.

The boundary displacement is found to correlate strongly with the plasma rotation. Whilst the boundary displacement in the presence of the LLM is usually sub-cm, it can become as large as 4 cm at very low plasma rotation, though in a large majority of cases this does result in plasma disruption. Figure 4 shows the boundary displacement measured in MAST as a function of the plasma rotation at the radial position of the minimum in safety factor for non-disruptive cases. The radial position of q_{min} varies between shots but is typically around mid-radius; figure 3 shows that the rotation profile is flattened in the presence of the LLM so the rotation at q_{min} is similar to that at the plasma axis. Here the boundary displacement is measured using visible imaging. For a few points, the measurement is taken as the average of the visible imaging and that from the Thomson scattering, which provides complementary data only when the diagnostic lasers were used in burst mode and sep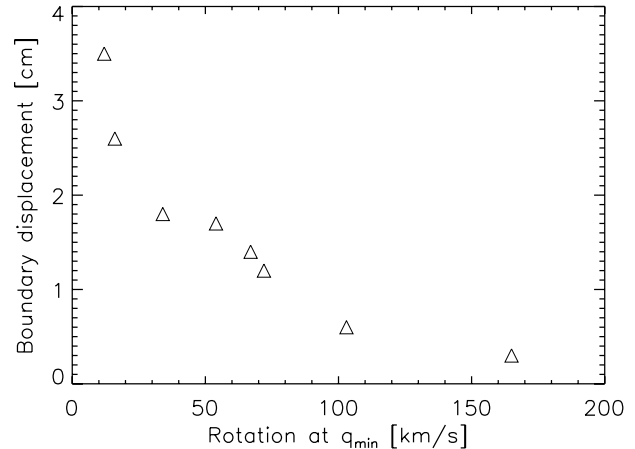arated by only a few μs, making it possible to resolve the distortion associated with the high-frequency LLM oscillation. Whilst it was shown that the rotation does not strongly influence the linear growth rate of the $n = 1$ kink mode in [1], these simulations do not account for the effect of the non-linear saturated state nor the interaction between the NTV braking and the mode evolution. In MAST, a temporal evolution is thus seen to occur: The mode onset occurs as the safety factor approaches unity [1]; the saturated kink mode then leads to a significant non-axisymmetry in the core, giving rise to neoclassical viscous braking torque [20]; the torque results in a reduction in the rotation in the plasma core where the mode is located, at which point the boundary displacement associated with the core instability is exacerbated. This means that for accurate prediction in ITER, non-linear modelling which includes the braking associated with the non-axisymmetry introduced by core MHD is needed.

Since ITER is likely to rotate at much slower velocities than present-day machines, one could infer from figure 4 that the edge displacement due to saturated $n = m = 1$ kink modes, as likely with broad low-shear q-profiles [26], may be large. However, it should be noted that in the spherical tokamak, the position of the minimum in safety factor is very broad. To investigate the edge displacement in a conventional aspect-ratio machine, the corrugation due to core MHD in hybrid plasmas in JET [2, 3] has been investigated. Across a database of JET hybrid plasmas, the spontaneously occurring continuous $n = m = 1$ ideal kink mode, which often occurs with the characteristic low-shear q-profile, never causes a discernible edge displacement. This is exemplified by figure 5, where a typical JET hybrid discharge, shot 84692, is shown to have a long-lasting $n = 1$ kink mode, but no change in the outer gap between the plasma edge and the wall measured by the fast magnetic signals. The only occasion when non-transient boundary displacements are observed is when a large ELM event (see [27]) triggers an $n = 1$ mode, with the plasma control system taking approximately an energy confinement time to recover the desired boundary position. An example of this is shown in figure 5.

Systematically, the saturated internal kink modes observed in MAST, JET and NSTX all lead to small boundary
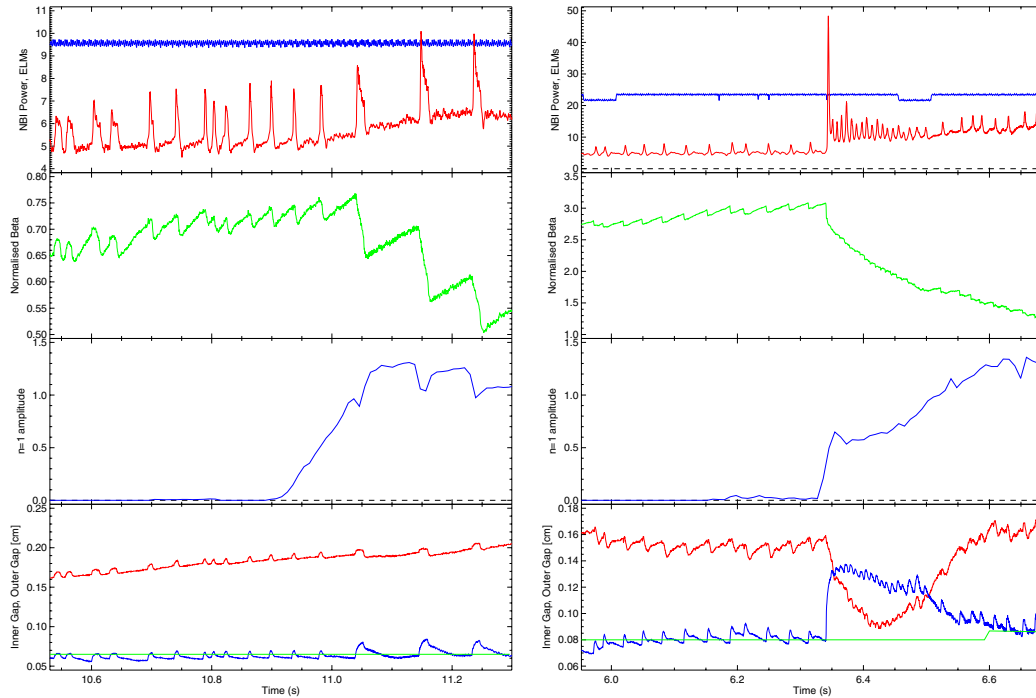
Figure 5. The NBI power and the total radiated power measured by the bolometer (showing the ELMs); (second pane) the normalized pressure, β_N; (third pane) the mode amplitude found from magnetics; and (fourth pane), the inner gap (red) and outer gap (blue) from EFIT reconstruction using fast magnetics, compared to the requested outer plasma position (green) used in the plasma control system. On the left is JET shot 84692 which has a long-lasting $n = 1$ kink mode, and on the right is shot 83521 which has an $n = 1$ kink mode triggered by a large ELM event.

displacements, as exemplified by figures 1 and 5(a). There are circumstances in both spherical tori and conventional aspect-ratio machines where these saturated kinks can lead to larger transient displacements, namely when strong rotation braking occurs (see figure 4 in MAST) or when triggered by a large ELM event (see figure 5(b) in JET). However, routinely the displacements from core saturated modes are sub-cm, meaning that the expectation for ITER is that should such saturated instabilities occur, the boundary perturbations will be tolerable.

2.2. NTMs and external $n = 1$ kink modes

Large displacements are also measured in the case of less core-localized MHD instabilities. High normalized pressure plasmas often exhibit saturated global $n = 1$ kink instabilities, or RWMs, which can persist for long times in the presence of magnetic feedback [14]. Whilst this low frequency mode activity is global and perturbs the plasma core, it also gives rise to significant shifts of the plasma boundary. Figure 6 shows the plasma boundary in NSTX, again diagnosed by the SXR camera, showing a displacement of ± 0.95 cm, or $\pm 1.6\%$ of the minor radius, when there is a saturated $n = 1$ kink mode in a high β_N plasma.

Naively one might expect the distortion to scale with the normalized pressure as the fluid drive for the instability is increased. However, there is no correlation between the boundary displacement in the presence of such global $n = 1$ instabilities and the normalized pressure with respect to the no-wall limit. Figure 7 illustrates how the plasma edge distortion measured in NSTX varies as the normalized pressure is varied from $\beta_N = 4.3$ to $\beta_N = 6$, above the no-wall stability limit.
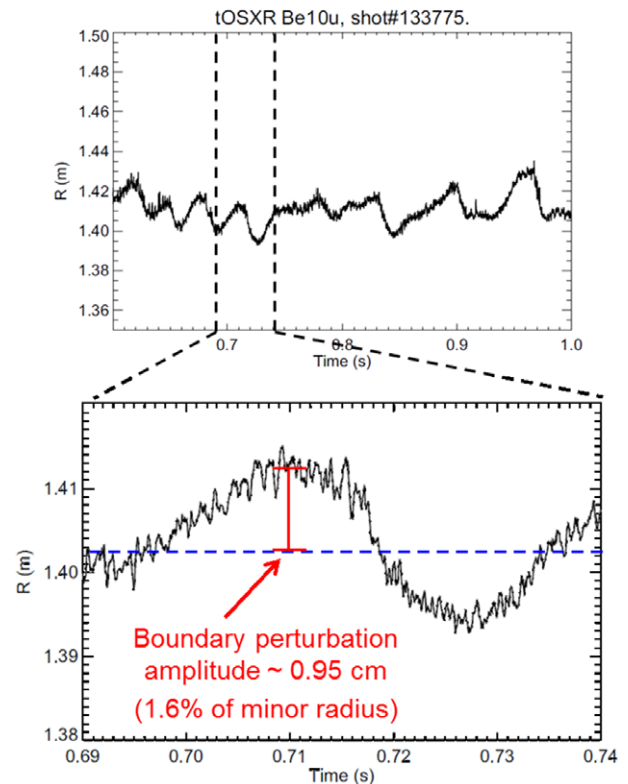

Figure 6. The plasma boundary measured by the ME-SXR system in NSTX for a discharge with an $n = 1$ external kink/RWM, showing a displacement of 1.6% of the minor radius.
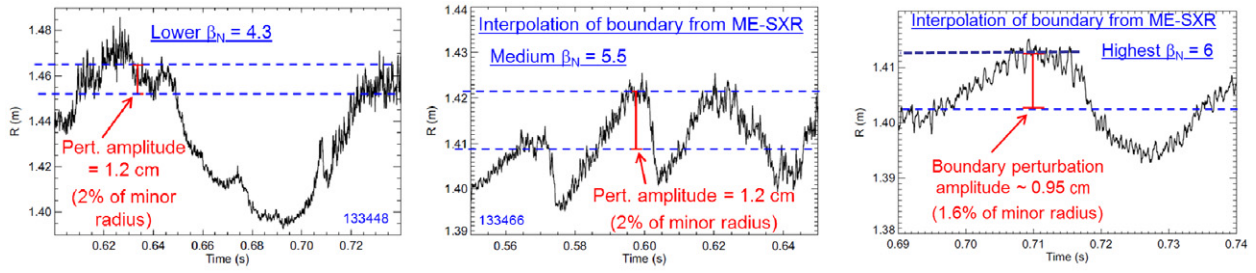
Figure 7. The plasma boundary measured by the ME-SXR system in NSTX for a discharge with an $n = 1$ external kink/RWM at (left) $\beta_{\mathrm N}$ less than the no-wall limit, (middle) intermediate normalized pressure and (right) for high $\beta_{\mathrm N}$ above the no-wall limit. The blue lines are to guide the eye to see the peak and median of the oscillation.
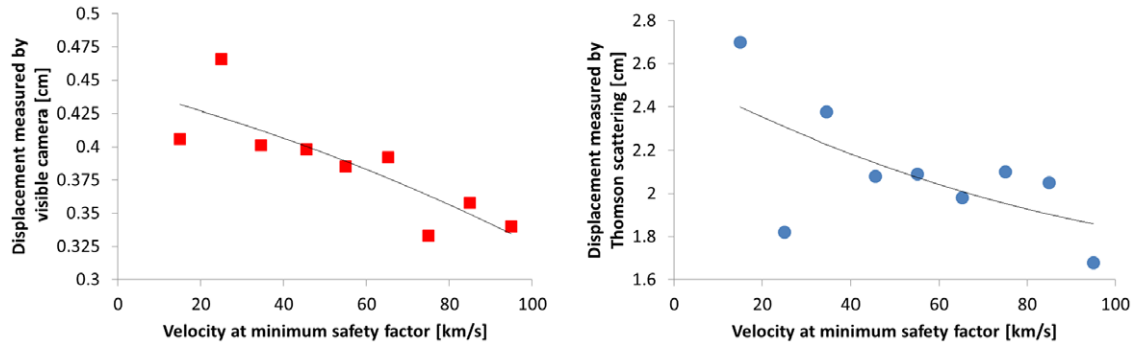

Figure 8. The edge displacement due to NTMs in MAST as measured by (left) the linear D_α camera and (right) Thomson scattering, as a function of the toroidal velocity of the plasma, showing that the boundary shifts increase as the rotation decreases. Second-order polynomials of best-fit are shown to guide the eye.

Note that the large excursion in boundary position for $\beta_{\mathrm N} = 4.3$ between $t = 0.65$–0.72 s is due to a temporary back-transition to L-mode caused by the mode. Figure 7 shows that the edge displacement is largely independent of $\beta_{\mathrm N}$. Actually, this is not unexpected since it has been shown that RWM stability depends sensitively on rotation and l_i as well as normalized pressure, and often plasmas at intermediate levels of rotation (i.e. neither the fastest nor slowest rotating cases in NSTX, nor the plasmas with highest NBI-driven $\beta_{\mathrm N}$) have the least stable modes as the kinetic damping is minimized [14, 28].

Conversely, MAST plasmas below the no-wall limit exhibit a strong dependence of the edge displacement on the plasma rotation. Linear CCD cameras have been used to measure D_α light generated by plasma electron impact excitation of the neutral gas outside the separatrix. These midplane cameras are oriented so that the pixel array can see the plasma boundary on both the high- and low-field side. There is some uncertainty in the position of the edge of the plasma inferred from the peak of the D_α emission [29] though qualitative differences between the different phases of the rotating mode are reliable. The Thomson scattering system on MAST [30] has a radial resolution <0.1 cm allowing detailed diagnosis of the electron density and temperature profiles. It was designed to achieve low systematic and random errors, allowing observation of changes in the gradients over narrow regions such as the edge pedestal. The displacement as measured by the D_α camera or the Thomson scattering clearly increases as the plasma rotation falls. Figure 8 shows the edge displacement due to NTMs as a function of the core plasma rotation velocity, illustrating largest boundary shifts for the slowest rotating plasmas.

3. Modelling of displacements due to core MHD in present machines

Saturated core instabilities such as those shown in section 2.1 can be modelled using three-dimensional equilibrium codes, where the naturally occurring helical core solution of a 3D equilibrium code is essentially the same as that from a non-linear MHD code (departing from an initially axisymmetric equilibrium) [7]. The ANIMEC code [31] (an anisotropic version of the ideal 3D equilibrium code, VMEC [32]) has been used to simulate the boundary displacements expected in MAST when a helically displaced core is found in the equilibrium solution. Providing a reversed shear q-profile is used, and providing $q_{\min}$ is sufficiently close to unity, two equilibria are found: one axisymmetric equilibrium, and the other a helical equilibrium with dominant $m = n = 1$ structure [7, 26, 33, 34]. The three-dimensional, helical equilibrium can have slightly lower energy than its axisymmetric neighbour, and so it is in this sense, a preferred state. One can consider the saturated state of a non-linear MHD code equivalent to a 3D equilibrium [7]. This is exemplified by figure 9 which, for $q_{\min} \geqslant 1$, shows good agreement of the amplitude of the core displacement due to an $n = 1$ kink mode in a low-shear $q \geqslant 1$ 'hybrid' scenario as found by a two-fluid non-linear MHD code, XTOR-2F [8], compared to that found in a 3D equilibrium analysis using ANIMEC. For $q_{\min}$ well below unity, despite the internal kink mode being unstable, as expected for the standard internal kink mode due to sufficient pressure drive [9], ANIMEC does not find a corresponding 3D equilibrium. This could be due to the different treatment of current sheets in ANIMEC and XTOR-2F code, and is an issue for future work. Nevertheless, it is
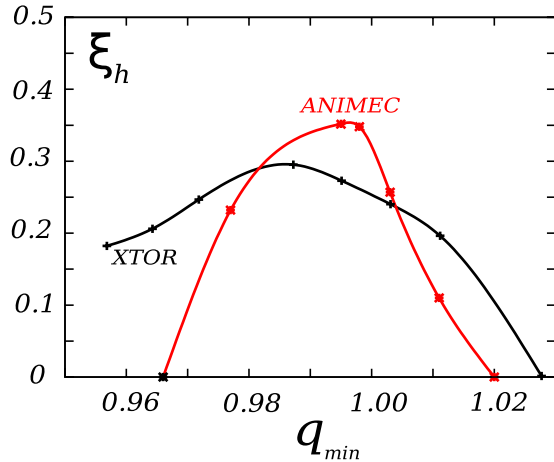
Figure 9. The displacement of the axis in ITER hybrid scenario as a fraction of the minor radius as a function of the minimum safety factor as predicted by non-linear MHD code, XTOR-2F, showing good agreement with 3D equilibria produced by ANIMEC.
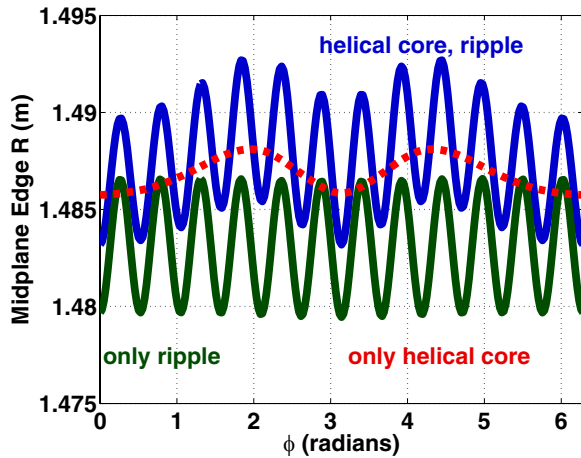

Figure 10. The midplane boundary position as a function of toroidal angle as modelled with ANIMEC for a MAST plasma with toroidal field ripple (green), a helical core (red), or both ripple and a helical core (blue).

reassuring to see the clear coincidence in the qualitative results from the two approaches for $q_{min} \geqslant 1$, suggesting that the two approaches are tantamount to one another under this condition.

The midplane boundary position predicted by ANIMEC is shown as a function of toroidal angle for a MAST plasma which exhibits a long-lived core kink mode [1] in figure 10. It is evident that the edge displacement caused by the core non-axisymmetry is negligible, and indeed smaller than the corrugation due to toroidal field ripple, which itself is much smaller than the perturbation due to applied resonant magnetic perturbations used for controlling edge localized modes [35].

Figure 11 exemplifies the relative insensitivity of the boundary displacement to the amplitude of the helical core, as parametrized by the value of q_{min} which dictates the susceptibility of the equilibrium to a non-axisymmetric branch. The boundary corrugation is of similar amplitude despite the helical core amplitude varying. Note that this equilibrium has an exaggerated bootstrap current in order to amplify the edge displacement [36] so that it is visible on the same scale as the helically displaced core, such that its invariance with

core displacement (or q_{min}) is observable. The equilibrium is most susceptible to an internal kink for q_{min} just above unity [36], and for $q_0 = 0.96, 1.05$ the saturated kink mode amplitude is smaller, yet the boundary displacement is relatively unchanged. The amplitude of the boundary displacement predicted by 3D equilibrium reconstruction exhibiting a helically displaced plasma core is in good agreement with that measured in the presence of a saturated kink mode. Furthermore, the boundary displacement is largely independent of the plasma pressure or the exact value of q_{min} (provided of course that q_{min} is in the range for which a helical core equilibrium is found), as also seen in the experimental data. However, there is a strong dependence of the edge displacement on the edge current [36], which is not borne out experimentally, as the boundary shift is insensitive to the pedestal temperature, and hence bootstrap current.

Similar saturated core instabilities can be analysed using non-linear MHD codes. Such non-linear MHD simulation has been performed using the two-fluid M3D-C¹ code [37] for an NSTX plasma which exhibits a saturated core kink instability [38] (such as that which gives rise to the boundary displacement shown in figure 1). Figure 12 shows the electron temperature profiles before the onset of the kink mode compared to a time when the mode has a saturated amplitude. It is clear that whilst the core of the plasma is cooled and deformed by the saturated kink mode, the boundary is negligibly affected. This is in good agreement with the measured displacement in NSTX (figure 1) which is less than 1 cm.

It should be noted that the simulations presented here are for non-rotating plasmas, whereas figure 4 shows that the displacement caused by a saturated $n/m = 1/1$ kink in MAST strongly depends on the plasma rotation velocity. Simulations of 3D equilibria with toroidal flows included will be the subject of future work.

4. Modelling of displacements due to core MHD in ITER

As discussed in section 2, the plasma scenario which is most prone to long-lasting saturated MHD is the so-called 'hybrid' or advanced inductive scenario due to the broad, low-shear region in the q-profile and higher normalized pressure. Of course, the baseline scenario is expected to experience MHD instabilities in the core, notably sawtooth oscillations, which could give rise to neoclassical tearing modes, both of which can lead to displacements of the plasma boundary. However, in the case of sawteeth the displacements are small and transient, and for NTMs the confinement degradation is a much more serious issue than whether the boundary is deformed. In comparison, the saturated core MHD experienced in hybrid plasmas is usually not overtly detrimental to the plasma performance in large aspect ratio tokamaks, but can last for many energy confinement times, and can lead to enduring displacements of the boundary which could result in difficulties for the plasma control system or for cycling of heat loads on plasma-facing components. Therefore, it is the boundary corrugation experienced in the ITER hybrid scenario which we analyse numerically in this section.

The current density profile used in ANIMEC has been tailored in order to give a slightly reversed shear safety
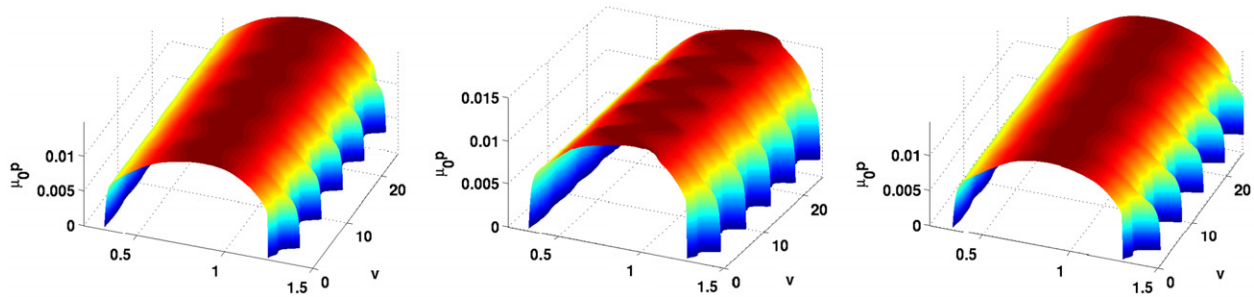
Figure 11. The plasma pressure as a function of radius and toroidal angle as modelled by ANIMEC for MAST plasmas with (left) $q_0 = 1.05$, (centre) $q_0 = 1.00$ and (right) $q_0 = 0.96$. In all cases there is a helical core, although its amplitude is maximized for $q_0 = 1.0$ and a corresponding boundary displacement.
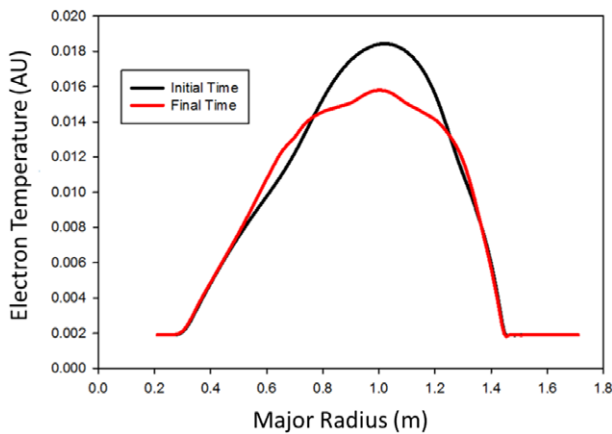

Figure 12. The electron temperature profiles in M3D-C[1] simulations of an NSTX plasma exhibiting a core kink instability, showing a large core displacement, but negligible change in the boundary position.

factor profile, though actually, the reverse shear is not a strong constraint on the results presented here and qualitatively similar results would be obtained for a flat, low-shear profile provided $q_{min} \approx 1$. Figure 13 shows the plasma pressure for the hybrid scenario equilibrium generated by ANIMEC for the axisymmetric branch, whilst figure 14 shows the pressure for a helical core branch of the equilibrium. It is clear that although the edge flux surfaces are barely perturbed, the plasma core can be significantly distorted when there is an $n = m = 1$ kink in the plasma core. Such a helical core would be expected to manifest itself as the long-lasting ideal perturbations observed in such 'hybrid' scenarios in MAST [1], JET [2], NSTX [4], TCV [6, 7] and EAST [5].

This boundary displacement in the presence of an $n = m = 1$ helical core is illustrated clearly in figure 15 where it can be seen that the two neighbouring states of equilibria found with ANIMEC lead to very different toroidal dependence of the plasma boundary. In the axisymmetric equilibrium, there is no corrugation of the boundary, whereas the helical core state, which is equally energetically favourable, gives rise to a ± 3 cm $n = 1$ distortion of the boundary. In both cases, toroidal field ripple is inherently included in the simulation, but the resultant boundary corrugation is negligibly small.

A comparable analysis has been performed using the non-linear MHD code, M3D-C[1]. It is worth recalling that the saturated state of an MHD instability found from an axisymmetric equilibrium is tantamount to a 3D equilibrium state for these hybrid profiles, as shown in figure 9 and [7] for the case of a fixed boundary. The electron temperature perturbation predicted by M3D-C[1] at different toroidal positions for the ITER hybrid scenario with realistic bootstrap current is shown in figure 16. Whilst there is a large $n = 1$ perturbation in the plasma core, there is negligible change in the position of the plasma boundary.

We have used both non-linear MHD modelling and 3D equilibrium modelling in order to predict the likely displacements in ITER due to saturated core modes. It has been shown [7] that these two approaches give similar magnitude of displacements and qualitatively the same trends as the safety factor is varied above unity. Indeed, figure 9 shows that for an ITER hybrid scenario with q_{min} just above one, the 3D equilibrium approach results in a similar core disturbance as the saturated state achieved in non-linear MHD simulations. This is also evident comparing the core perturbation from figure 15 (right) with that in figure 16. This supports the notion that the core perturbation from the two approaches leads to similar results, despite solving very different equations. However, the boundary corrugation can be rather different, partially explicable by the treatment of the free boundary conditions. In M3D-C[1], the fields external to the plasma are held constant on a surface that approximates the ITER vacuum vessel, whereas in ANIMEC, the perturbed fields are allowed to extend to infinity. In order to verify these modelling approaches, in section 3 they have been applied to present-day devices with good quantitative agreement: M3D-C[1] and ANIMEC have been applied to NSTX and MAST plasmas respectively, and accurately predict sub-cm boundary displacements in the presence of saturated core instabilities, as is observed empirically. There remain uncertainties in the modelling, not least the effect of toroidal rotation and behaviours with safety factor below unity (exemplified by figures 4 and 9 respectively) as well as the boundary conditions, and these will be subject of future work. Due to these inherent uncertainties it is not possible to make firm predictions for the exact amplitude of the displacement likely in ITER due to saturated core instabilities. That said, the predicted displacement in ITER hybrid scenarios due to saturated kink modes prevalent with low shear and $q_{min} \approx 1$ is in the range <1 cm (M3D-C[1]) to 3 cm (ANIMEC) equating to a relative displacement of ± 0–1.5% of the minor radius. Whilst this is not insignificant, it is well within the acceptable bounds of the boundary displacement allowable in ITER for both
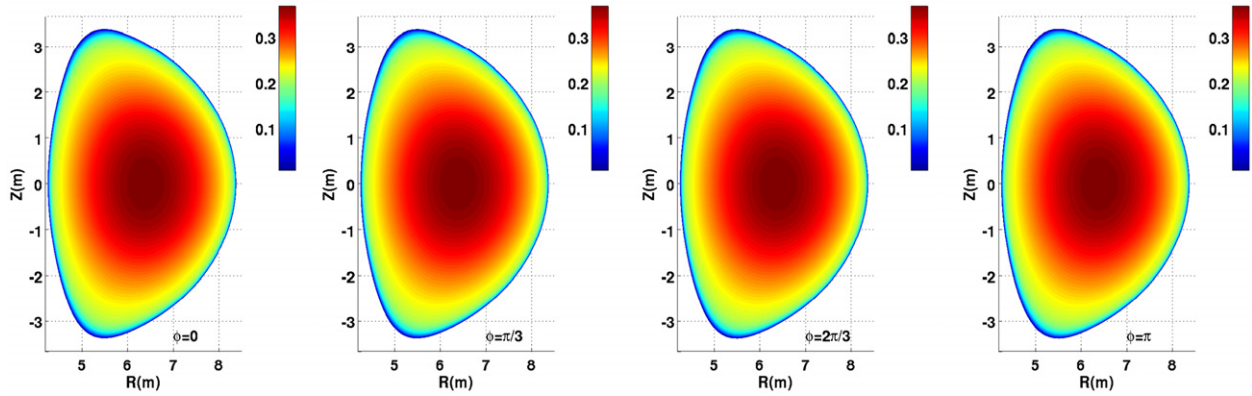
Figure 13. Poloidal cross-section plots of $\mu_0 P (H Pa/m)$ for the ITER hybrid scenario as predicted by ANIMEC for the axisymmetric equilibrium branch at $\phi = 0, \pi/3, 2\pi/3, \pi$.
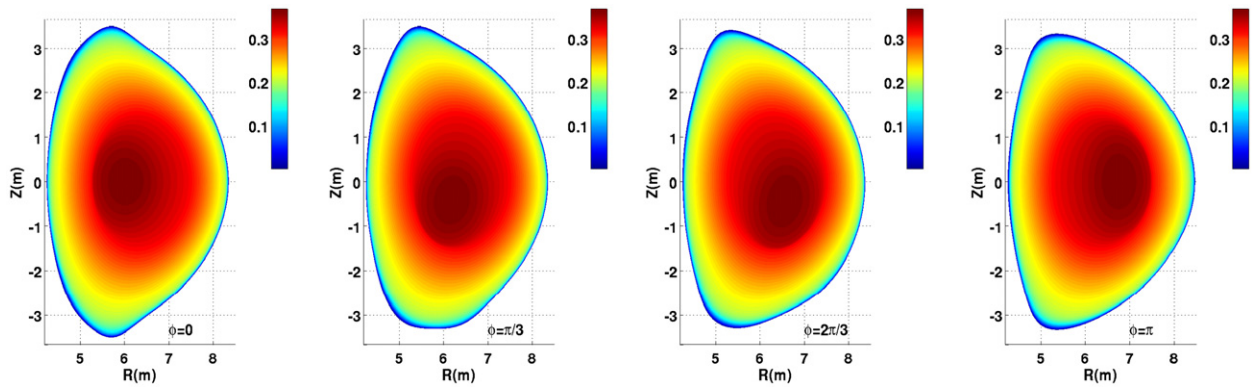

Figure 14. Poloidal cross-section plots of $\mu_0 P (H Pa/m)$ for the ITER hybrid scenario as predicted by ANIMEC for the helical core branch at $\phi = 0, \pi/3, 2\pi/3, \pi$.
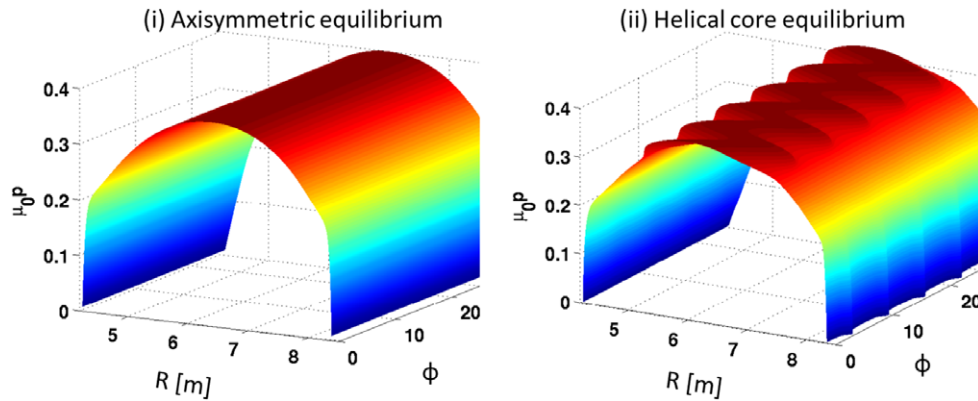

Figure 15. The plasma pressure as a function of radius and time for (left) the axisymmetric case and (right) the helically displaced core for the ITER hybrid scenario, showing the $n = 1$ helical core and the perturbation to the edge position.

plasma control to be effective and heat loads to the plasma-facing components to be manageable, suggesting that despite the remaining uncertainty in the models, the displacements in ITER will be tolerable.

5. Discussion and conclusions

It is evident that saturated MHD instabilities can give rise to significant displacements of the plasma boundary. These displacements have been measured in various tokamaks and successfully compared with numerical simulation,

notwithstanding the approximation of static plasmas, whilst the rotation is seen empirically to affect the edge plasma displacement caused by saturated kink modes. Good agreement has been found between these experimental measurements and numerical simulation—either ideal three-dimensional MHD equilibrium reconstruction or non-linear MHD modelling—giving credence to the application of such simulations for extrapolation to ITER. The boundary displacement resultant from core MHD instabilities in ITER is predicted to be less than $\pm 1.5\%$ of the minor radius.

Such toroidal corrugation of the plasma boundary affects many things, notably the coupling of ICRH, the minimum
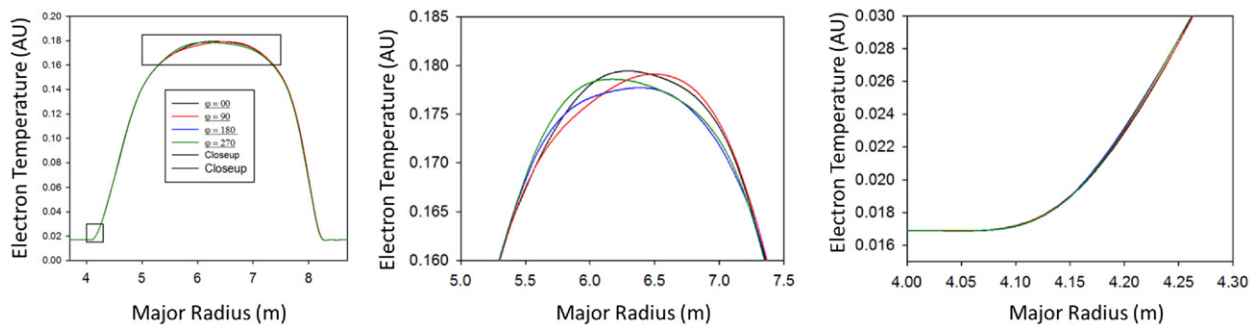
Figure 16. The electron temperature profile at four different toroidal positions for an ITER hybrid plasma as predicted by the M3D-C^1 code for (left) the whole major radius, (centre) the core plasma showing an $n = 1$ kink mode and (right) the pedestal, showing negligible boundary displacement.

values of wall gaps assumed for safe operation, the plasma position control and the control of ELMs. Whilst a displacement of ± 3 cm in the baseline scenario is allowable from both a plasma control and heat loading perspective, it is important to realize that such displacements may occur and plan for the plasma control system and heating actuators to be able to account for such distortions safely.

Acknowledgments

References

[1] Chapman I.T. *et al* 2010 *Nucl. Fusion* **50** 045007
[2] Buratti P. *et al* 2010 *Nucl. Fusion* **52** 023006
[3] Kwon O.J. *et al* 2012 *Plasma Phys. Control. Fusion* **54** 045010
[4] Menard J.E. *et al* 2006 *Phys. Rev. Lett.* **97** 095002
[5] Chen W. *et al* 2010 *Nucl. Fusion* **50** 084008
[6] Reimerdes H. *et al* 2006 *Plasma Phys. Control. Fusion* **42** 629
[7] Graves J.P. *et al* 2013 *Plasma Phys. Control. Fusion* **55** 014005
[8] Lütjens H., Luciani J.-F., Leblond D., Halpern F. and Maget P. 2009 *Plasma Phys. Control. Fusion* **51** 124038
[9] Bussac M.N., Pellat R., Edery D. and Soule J.L. 1975 *Phys. Rev. Lett.* **35** 1638
[10] Baruzzo M. *et al* 2010 *Plasma Phys. Control. Fusion* **52** 075001
[11] La Haye R.J. *et al* 2002 *Phys. Plasmas* **9** 2051
[12] Maraschek M. *et al* 2003 *Plasma Phys. Control. Fusion* **45** 1369
[13] Garofalo A.M. *et al* 2007 *Nucl. Fusion* **49** 1121
[14] Sabbagh S.A. *et al* 2010 *Nucl. Fusion* **50** 025020
[15] Katsuro-Hopkins O. *et al* 2007 *Nucl. Fusion* **47** 1157
[16] Bolzonella T. *et al* 2008 *Phys. Rev. Lett.* **101** 165003
[17] Kocan M. 2013 Heat loads to the ITER first-wall panels in the ICRH-optimized plasma equilibrium *Technical Report* ITER DML5YK
[18] Lister J.B., Portone A. and Gribov Y. 2006 *Control. Syst.* **26** 79
[19] Menard J.E. *et al* 2005 *Nucl. Fusion* **45** 539
[20] Hua M.D. *et al* 2010 *Eur. Phys. Lett.* **90** 55001
[21] Cooper W.A. *et al* 2013 *Nucl. Fusion* **53** 073021
[22] Hua M.D. *et al* 2010 *Plasma Phys. Control. Fusion* **52** 035009
[23] Shaing K.C. 2003 *Phys. Plasmas* **10** 1443
[24] Avinash, Hastie R.J., Taylor J.B. and Cowley S.C. 1987 *Phys. Rev. Lett.* **59** 2647
[25] Rosenbluth M.N. *et al* 1973 *Phys. Fluids* **16** 1894
[26] Cooper W.A. *et al* 2011 *Plasma Phys. Control. Fusion* **53** 024002
[27] Baranov Y.F. *et al* 2012 *Nucl. Fusion* **52** 023018
[28] Berkery J.W. *et al* 2010 *Phys. Rev. Lett.* **104** 035003
[29] Tournianski M.R. *et al* 2003 *Rev. Sci. Instrum.* **74** 2089
[30] Scannell R. *et al* 2008 *Rev. Sci. Instrum.* **79** 10E730
[31] Cooper W.A. *et al* 2009 *Comput. Phys. Commun.* **180** 1524
[32] Hirshman S.P. and Lee D.K. 1986 *Comput. Phys. Commun.* **43** 143
[33] Cooper W.A. *et al* 2011 *Plasma Phys. Control. Fusion* **53** 074008
[34] Cooper W.A. *et al* 2011 *Plasma Phys. Control. Fusion* **53** 124005
[35] Chapman I.T. *et al* 2012 *Plasma Phys Control Fusion* **54** 105013
[36] Cooper W.A. *et al* 2013 *40th EPS Conf. on Plasma Physics (Helsinki, Finland, 2013)* http://eps2013.aalto.fi
[37] Jardin S.C., Breslau J. and Ferraro N. 2007 *J. Comput. Phys.* **226** 2146
[38] Breslau J.A. *et al* 2011 *Nucl. Fusion* **51** 063027